Clinical Imaging 58 (2019) 59–65

Contents lists available at ScienceDirect

Clinical Imaging

journal homepage: www.elsevier.com/locate/clinimag

Pediatric Radiology

Imaging findings in epithelioid hemangioendothelioma

Yan Epelboym[a], Dawn R Engelkemier[a], Frederic Thomas-Chausse[a], Ahmad I. Alomari[a,d], Alyaa Al-Ibraheemi[b,d], Cameron C. Trenor III[c,d], Denise M. Adams[c,d], Gulraiz Chaudry[a,d,*]

[a] Division of Vascular and Interventional Radiology, Boston Children's Hospital and Harvard Medical School, United States of America
[b] Department of Pathology, Boston Children's Hospital and Harvard Medical School, United States of America
[c] Division of Hematology/Oncology, Boston Children's Hospital and Harvard Medical School, United States of America
[d] Vascular Anomalies Center, Boston Children's Hospital and Harvard Medical School, United States of America

ARTICLE INFO

Keywords:
Radiology
Epithelioid hemangioendothelioma
Pediatrics

ABSTRACT

Purpose-objective: Epithelioid hemangioendothelioma (EHE) is a rare vascular malignancy with varying biologic behavior. The purpose of this study was to identify imaging findings most characteristic of EHE.
Methods: Retrospective review of clinical and imaging records in patients referred to our Vascular Anomalies Center over a 17 year period with biopsy proven EHE.
Results: We evaluated 29 patients (17 F) with median age of 16 years (range 2–76 y). The most common presenting symptoms were pain (n = 13) and palpable mass (n = 7). 22 (70%) had multifocal disease. Most common sites of involvement were lung (n = 25), liver (n = 16), bone (n = 12), soft tissue (n = 3) and lymph nodes (n = 1). Of patients with single site disease, 3 had lung, 3 liver, and 1 had bone lesions. In 18/25 with lung disease, there were multiple nodules of varying sizes and characteristics. In 14/16 with hepatic disease there were multiple nodules with predominantly peripheral distribution. Subcapsular retraction was seen in 10/16 and a "lollipop" sign (hepatic or portal vein tapering at the edge of a well-defined hypoenhancing lesion) identified in 5/16. Of 12 osseous lesions, 11 were lytic, 8 involved vertebrae and 9 involved the axial skeleton.
Conclusion: EHE has varied imaging findings. The most common sites are lungs, liver, and bone, with multiorgan involvement seen in most. Lung disease is most commonly characterized by multiple nodules. Hepatic lesions demonstrate the most distinctive findings, with peripheral distribution, lack of early enhancement, subcapsular retraction and "lollipop" sign. Osseous lesions are commonly lytic and more prevalent in the axial skeleton.

1. Introduction

Epithelioid hemangioendothelioma (EHE) is a rare vascular malignancy with intermediate behavior between that of benign hemangioma and malignant angiosarcoma [1,2]. The entity was first described in the soft tissues in 1982 by Weiss and Enzinger who evaluated 41 cases of solid tumors of vascular origin with "epithelioid" or "histiocytoid" endothelial cells [3]. The presentation, clinical course, and imaging appearance of EHE are variable, and its rarity adds to the challenge of diagnosis. The purpose of this study was to review the imaging findings in patients with biopsy proven EHE and identify features most characteristic of the disease.

2. Materials and methods

In this institutional review board approved, Health Insurance Portability and Accountability Act compliant retrospective study, informed consent was waived.

Imaging and clinical records were reviewed in patients that were referred to our Vascular Anomalies Center between 2001 and 2018 with a histologically proven diagnosis with EHE. Only patients with radiological studies were included. The imaging findings were evaluated independently by 4 radiologists (YE, DE, FTC, GC) and discrepancies resolved by consensus by at least 2 of the readers. Patient demographics and presenting symptoms were recorded. When more than one imaging study was available, the earliest study was used for initial evaluation and compared to subsequent studies to evaluate temporal progression as evidenced by changing size and/or number of lesions. Site of involvement and pattern of lesion distribution were recorded.

Within the lung, the pattern of distribution was documented as solitary or multiple pulmonary nodules. Nodules were classified as solid or ground-glass. Ground-glass nodules were defined as subsolid nodules

* Corresponding author at: Boston Children's Hospital and Harvard Medical School, 300 Longwood Ave, Boston, MA 02115, United States of America.
E-mail address: gulraiz.chaudry@childrens.harvard.edu (G. Chaudry).

https://doi.org/10.1016/j.clinimag.2019.06.002
Received 12 March 2019; Received in revised form 28 May 2019; Accepted 11 June 2019

that were either pure ground glass or part solid. Images were evaluated for associated pleural thickening and effusion.

In the liver, the location of lesions was classified as subcapsular if the lesion abutted the capsule, peripheral if the lesion was within 2 cm of the capsule but not adjacent to the capsule, or central if the lesion was greater than 2 cm from the capsule. Associated capsular retraction was documented. Evaluation for the presence of a hepatic or portal vein tapering at or along the periphery of a well-defined peripherally enhancing lesion, the previously described "lollipop sign," [4] was conducted.

Osseous lesions were evaluated for pattern of bone destruction, reactive sclerosis, periosteal reaction, cortical thinning, cortical expansion, and associated soft tissue involvement.

3. Results

3.1. Clinical characteristics

There were a total of 29 patients (17 F) with a histologic diagnosis of EHE. The median age at presentation was 16 years (range 2–76 years). Sixteen of the patients were less than 18 years of age, likely because our institution is a pediatric referral center. The most common presenting symptoms were pain (n = 13), mass (n = 7), and constitutional symptoms of fatigue and malaise (n = 2); eight patients were asymptomatic (Table 1). Twenty-two patients had multi-organ involvement. The most commonly affected organs were lung (n = 25), liver (n = 16), and bone (n = 12). Less frequent sites of involvement included skin and subcutaneous tissues [3] and lymph nodes [1].

3.2. Imaging findings

3.2.1. Lung

CT of the chest was available in all patients with reported lung involvement. During follow-up an MRI of the chest was also performed in 3 patients. At initial presentation, the most common pattern of distribution was bilateral pulmonary nodules (18/25). Solid nodules were identified in 17 these patients (Fig. 1), with some ground glass nodules also seen in 7 of these patients. One patient had only ground-glass nodules at presentation (Fig. 2). Nodule size was variable, ranging from 1 to 39 mm. Six patients had a solitary solid pulmonary nodule. In 1 patient, the only chest finding was pleural thickening. Pleural thickening was also seen in one patient with multiple pulmonary nodules and a pleural effusion was identified in one patient with a solitary pulmonary nodule. A small pneumothorax was identified in 2 patients.

Twenty patients with lung findings had follow-up imaging available.

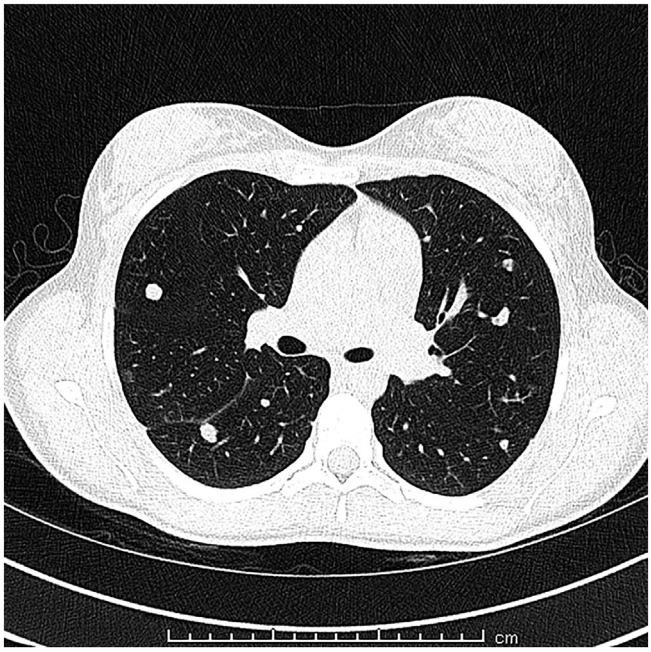

Fig. 1. 15-year-old female with pulmonary EHE. Axial CT scan of the chest. Multiple solid pulmonary nodules are seen bilaterally.

Table 1
Summary of clinical features.

Patient	Age at presentation (years)	Gender	Presenting symptom(s)	Sites of involvement	Biopsy site(s)
1	13	M	Fever, pain	Lung	Lung
2	13	M	Pain	Lung, bone	Bone -mandible/Lung
3	16	M	Palpable hard palate lesion	Lung, bone	Hard palate
4	76	M	Decreased appetite, pain	Liver	Liver
5	12	F	Facial mass	Lung, soft tissue	Soft tissue
6	42	F	Pain	Liver, lung	Liver
7	23	F	Asymptomatic	Liver, lung	Liver
8	59	F	Asymptomatic	Liver, lung, bone	Liver/Lung
9	16	M	Pain	Lung	Lung
10	29	F	Asymptomatic	Liver, lung	Liver
11	15	F	Shoulder/Hip Pain	Lung, bone	Lung
12	52	M	Constitutional symptoms, fatigue malaise	Liver, lung	Lung
13	62	F	Constitutional symptoms, nausea	Liver	Liver
14	15	F	Asymptomatic	Lung, bone	Lung
15	17	F	Pain	Lung, bone	Lung, bone
16	10	M	Pain	Liver, lung, soft tissue	Soft tissue, liver
17	51	F	Asymptomatic	Liver, lung, bone	Lung, Liver
18	13	M	Ankle pain	Bone	Bone
19	67	F	Asymptomatic	Lung	Lung
20	20	F	Pain	Liver, lung, bone	Liver
21	2	M	Palpable soft tissue mass	Lung, soft tissue	Soft tissue
22	7	F	Pain	Liver, Lung	Liver
23	30	F	Pain	Liver, lung	Liver
24	48	F	Asymptomatic	Liver	Liver
25	12	M	Pain	Lung, bone	Lung, bone
26	8	F	Pain	Lung, soft tissue	Soft tissue
27	10	M	Pain	Liver, lung	Liver
28	16	M	Asymptomatic	Liver, lung, bone	Lung, bone
29	24	F	Thigh mass	Liver, lung, bone, soft tissue	Bone, soft tissue

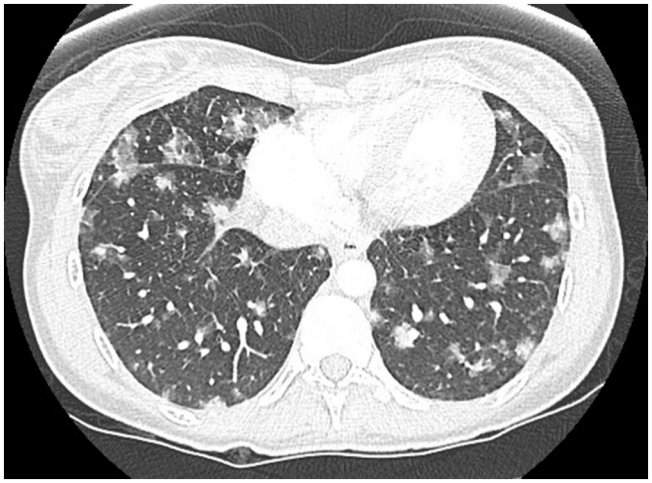

Fig. 2. 23-year-old female with pulmonary EHE. Axial CT scan of the chest. Multiple ground glass nodules are seen bilaterally.

Mean follow-up period was 2.9 years (0.5–8 years). In one patient, the solitary pulmonary nodule was resected. The disease was stable at the end of the follow-up period in 9 patients. In 10 patients, there was evidence of progressive disease, with increase in size and number of nodules in 3 and increase in size but not number in 3. Cavitation of the initial lesions was identified in 1 and progressive consolidation of the lung in 1. In one patient, there was increase in the extent of pleural disease. Progressive lung fibrosis was noted in 1 patient.

3.2.2. Liver

As a consequence of the fact that these patients were referred from other centers, the imaging modalities available for review were primarily cross-sectional. Fourteen of the 16 patients with reported liver involvement had CT imaging available and 7 had MRI imaging. Follow-up imaging was available in 12, with a mean follow-up period of 2.7 years (0.5–6 years). At initial presentation most (14/16) patients had multifocal lesions. In 13 of these 14 patients, the lesions were peripheral or subcapsular in location (Fig. 3). Eight patients had evidence of subcapsular retraction at initial imaging, with progressive worsening of retraction seen in 5 patients. Two patients with subcapsular nodules at initial imaging developed retraction over the follow-up period. One patient had a solitary lesion in a central location and one had a solitary peripheral lesion. Hepatic lesion size ranged from 4 to 67 mm at initial presentation.

A non-contrast study was performed in patient. The remainder had a portal venous phase study performed. In addition an arterial phase study was available in 3 and a delayed phase in 1. On CT the lesions were hypoattenuating compared to normal liver parenchyma in all patients. Following the administration of contrast, there was peripheral enhancement of one lesion in 1 patient and evidence of progressive filling in of the lesion in the patient that had a delayed study performed. In the remaining patients there was no evidence of enhancement on administration of contrast. Five patients had at least one lesion that demonstrated a classic “lollipop” sign on contrast enhanced CT (Fig. 4).

A PET-CT was performed in 4 patients with hepatic disease; avid uptake of radiotracer was seen in 3. In one patient there was increased uptake of radiotracer in some of the lesions, but not others.

On MRI, the lesions were hypointense on T1 and either uniformly hyperintense or had a targetoid appearance (3/7) on fluid-weighted sequences (Fig. 5). On administration of gadolinium, the most common pattern of enhancement was peripheral (5/7) or uniform (5/7); in some patients both types of enhancement patterns were seen within the multiple lesions. Delayed sequences were performed after contrast administration in 5 patients. In 4 of these, there was evidence of progressive filling in of the lesions that initially demonstrated peripheral

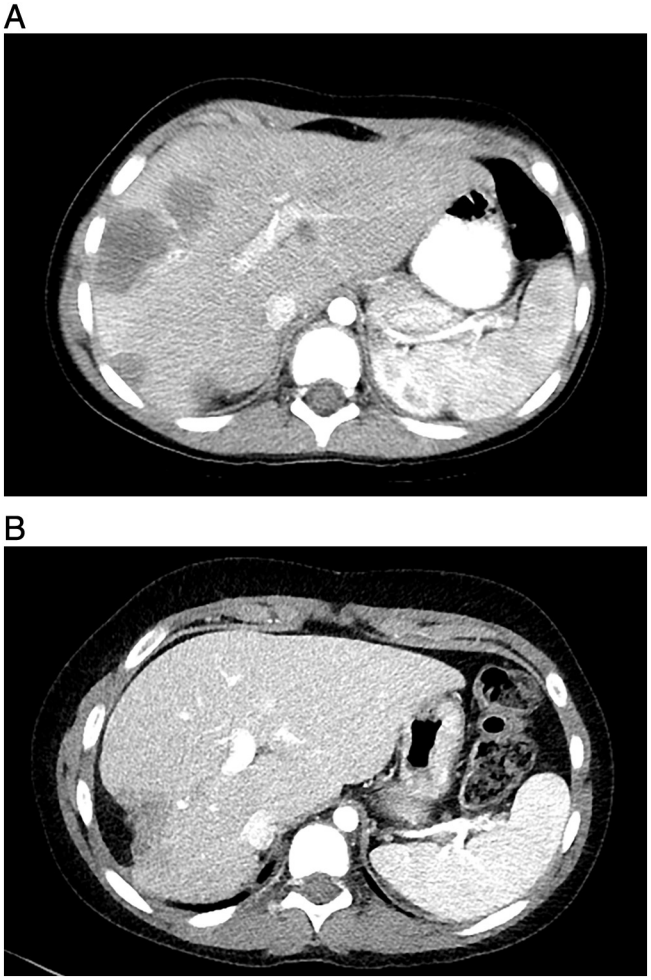

Fig. 3. 7-year-old girl with hepatic EHE. Axial contrast enhanced CT of the abdomen. (a) Multiple low attenuation hepatic lesions are seen. (b) Follow-up study performed 2 years later demonstrates subcapsular retraction in the right lobe.

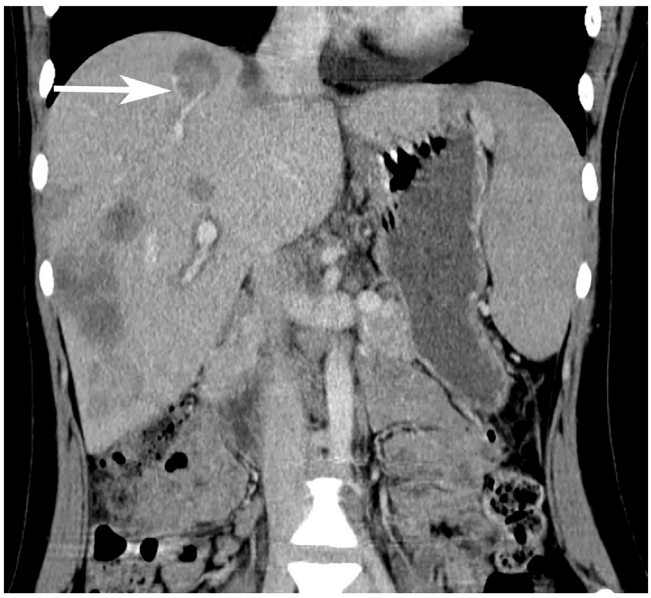

Fig. 4. 20-year-old female with hepatic EHE. Coronal contrast enhanced CT scan of the abdomen. There are multiple low attenuation hepatic lesions with a lollipop sign seen in the most superior lesion (arrow).

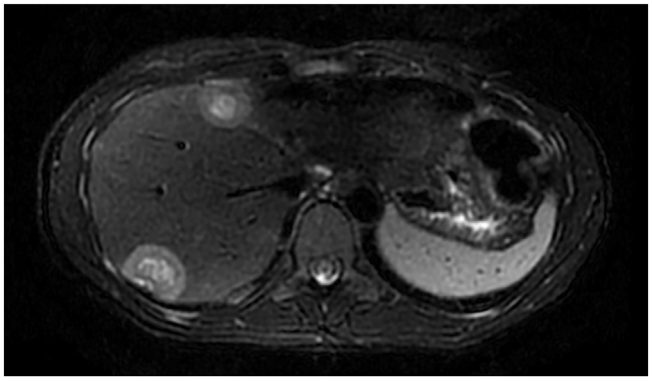

Fig. 5. 30-year-old female with hepatic EHE. Axial fat-saturated T2 MRI image. Two peripheral hepatic lesions are seen with a targetoid appearance.

enhancement.

3.2.3. Bone

CT was performed in all 12 patients with osseous lesions, with an MRI also available in 3 patients. Lytic lesions, some with a sclerotic rim, were identified in 11/12 with osseous disease at initial presentation (Fig. 6). The remaining patient had an expansile mixed lytic-sclerotic lesion. On MRI, the lesions were hypointense on T1 and hyperintense on T2/STIR sequences. The spine was the most common site of involvement (8/12) and disease was limited to the axial skeleton in 9/12. Six patients had solitary osseous lesions. The size of the osseous lesions ranged from 9 to 69 mm. An associated paravertebral soft tissue mass was seen in 1 patient. Plain radiographs were available in 7 of 12 patients. Two of these patients had lesions in the appendicular skeleton, which were well visualized as focal lytic areas with a sclerotic rim. The other 5 patients had lesions limited to the axial skeleton, which were either not seen or incompletely visualized on plain radiographs.

Follow-up imaging was available in 19 patients, with a mean follow-up period of 3.6 years (1.4–8 years). There was worsening of osseous disease in 3 patients, 2 with increase in size of the lesions and 1 with an increase in number and size.

3.2.4. Other sites of involvement

Imaging was available in 3 of 4 patients with skin and subcutaneous involvement; in the other patients only the post resection studies were available. The lesions were isointense to muscle on T1 and hyperintense on T2. A solitary area of involvement was seen in all, involving the scalp, upper extremity, groin and thigh. One patient with lymph node involvement had CT imaging available. This manifested as mild enlargement of multistation cervical lymph nodes.

3.2.5. Follow-up

Twenty-three patients had serial imaging available, which allowed evaluation of progression. Median follow up period was 2.7 years (range 0.5–8 years). Fourteen patients showed imaging evidence of progression over this period as evidence by increase size or number of lesions as detailed above. Clinical follow-up information was available in 18. Three patients died during the study period, 2 due to the underlying disease and one with unknown cause. One patient demonstrated stable disease for 17 months, followed by intractable progression of osseous and respiratory disease, resulting in death 3 years after presentation. The other patient also had progressive osseous and respiratory disease and died 2 years after presentation. There was no definite correlation with pattern of disease (organs involved, multi-organ involvement) and imaging or clinical progression.

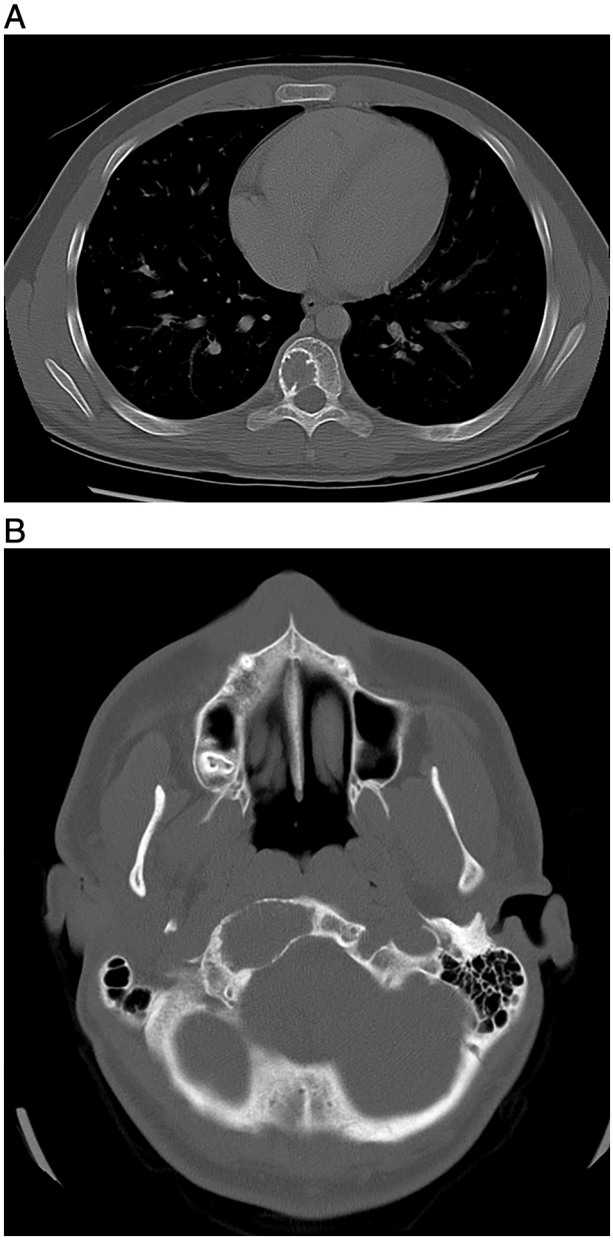

Fig. 6. 16-year-old boy with osseous EHE. Axial CT scan images on bone windows. (a) A lytic lesion with a sclerotic rim is seen in the right side of the vertebral body. (b) There is an expansile lytic lesion in the right occipital condyle.

3.3. Histopathology

All patients had histological confirmation of the diagnosis. The site biopsied was liver [12], soft tissue or bone [12] and lung [10]. More than one site was biopsied in 6.

At least one specimen from all patients had immunohistochemical staining performed for endothelial cells (CD31, CD34, and ERG). One specimen was stained for CAMTA1. TFE3 stain was performed on two specimens.

Histologically, all tumors consisted of epithelioid cells arranging in small nests, cords, and solid sheets in a variably myxoid to collagenized background (Fig. 7a). The lung and pleural biopsy typically showed multi focal involvement of small airspaces while the hepatic lesions showed mostly sinusoidal pattern. Lesional cells had round nuclei with voluminous eosinophilic cytoplasm, some of which had well-defined punched out intracytoplasmic lumina, some with a single red blood cell.

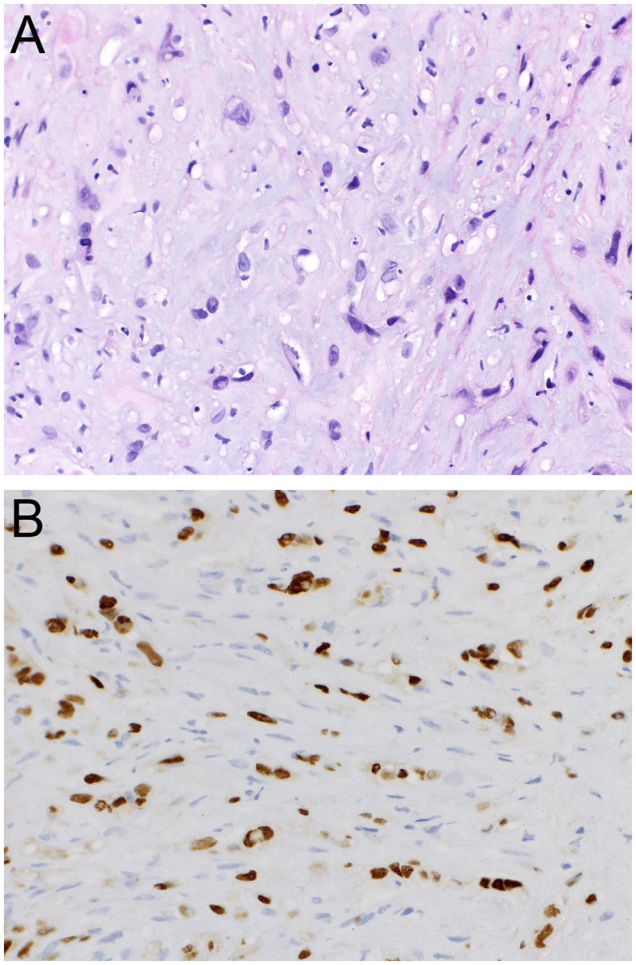

Fig. 7. (a) Histopathology of EHE typically showed epithelioid cells arranging in cords or single cells in a myxoid matrix, some cells contain intracytoplasmic lumina. (b) CAMTA1 immunohistochemistry showing nuclear positivity of tumor cells.

Pleomorphism was minimal. Necrosis was noted in two cases. Endothelial cells were positive for CD31 and variably for CD34 and Keratin. CAMTA1 stain was positive in one tested case (Fig. 7b). One case was positive for TFE3 and had vasoformative morphology, with well-formed blood vessels lined by epithelioid endothelial cells with abundant eosinophilic cytoplasm lacking cytologic atypia.

4. Discussion

EHE is a rare vascular neoplasm that arises from endothelial or pre-endothelial cells [1,2]. In part due to its low incidence (estimated 1 in 1 million), EHE is challenging to diagnose clinically, radiographically, and histologically [5,6]. Recent identification of specific oncogenic fusions has facilitated the diagnosis [8]. Most commonly identified (in 90–95% of cases) is the reciprocal translocation of WW domain-containing transcription factor 1 (WWTR1) and calmodulin transcription activator 1 (CAMTA1) [8]. CAMTA1 over-expression can be seen by immunohistochemistry, adding confidence to the histologic diagnosis [7,8]. EHE is commonly multifocal with involvement of multiple organs, particularly in children [7].

The presentation and clinical course of EHE are variable. EHE has been reported to be more common in females, particularly the hepatic and pulmonary forms [9]; however osseous and primary pleural involvement are more common in males [10]. In a registry of 206 adult patients, with a mean age of 38, the most common presenting symptom was found to be pain; however more than 25% of patients were asymptomatic, presenting as an incidental imaging or clinical finding [9]. Our series showed similar findings of a female gender predilection. Pain was the most common presenting symptom, but more than 50% presented with either a palpable mass or incidental findings on imaging.

While EHE may present in almost any location, it usually affects the soft tissues and visceral organs. As seen in our study, liver, lung, and bone are the most frequently affected organs. Less commonly, EHE may arise in lymph nodes [11], pleura [12], thyroid [13], omentum, mesentery, cutaneous tissues, and muscle [14,15]. Single organ involvement has most commonly been reported with hepatic disease [7], but in our cohort solitary pulmonary disease had a similar incidence.

Pulmonary EHE was first described in 1975 by Dail and Liebow as “intravascular bronchiolalveolar tumor” [16] and later recognized as a pulmonary counterpart to EHE in other sites [7]. Three patterns of pulmonary EHE have been described: multiple pulmonary nodules, multiple pulmonary reticulonodular opacities, and diffuse infiltrative pleural thickening [17]. Well-defined bilateral parenchymal nodules are the most common manifestation [3,9,17] and this pattern was also seen in our series. Reticulonodular opacities with interlobular septal thickening and ground glass opacity are less common [17]. This appearance has been attributed to intraluminal tumor cells within small blood and lymphatic vessels [18–20] and has been reported to have a poor prognosis [21]. Ground glass opacities were commonly seen in our cohort, but there was no definite correlation with disease progression. Diffuse smooth and nodular infiltrative pleural thickening, similar in appearance to that of pleural carcinomatosis or mesothelioma, usually has a more aggressive course as well [22,23]. There was rapid progression of the disease in 1 of our 2 patients with pleural disease. Solitary pulmonary nodules measuring up to 5 cm are reported in less than 10% of cases [19,24,25], but were seen in almost 25% of cases in our series. Although calcification and ossification are commonly seen on histologic specimens, visible calcification on imaging is not common, and was not seen in our series [18].

On CT, hepatic EHE usually manifests as multiple low attenuation nodules of variable size preferentially involving the subcapsular region. Early in the disease course, discrete multifocal nodules are present. Later, nodules coalesce to form confluent masses [26,27]. The relative low attenuation of the lesions compared to normal liver parenchyma is related to myxoid and hyalinized stroma [14]. Fibrosis in association with subcapsular tumors can result in capsular retraction [26,28]. Most of the patients in our series (10/17) developed progressive capsular retraction, which is similar to the 59.5% reported by Zhao et al. [29]. On post-contrast imaging, a target or halo pattern has been reported [28] while in others only mild peripheral enhancement may be visible [15,30]. Delayed post contrast imaging shows variable central enhancement or lack of enhancement depending on the degree of fibrosis, myxoid and hyalinized components [11,14,31]. In our series, on CT there was no enhancement of the lesions following administration of contrast. This may reflect the timing of the contrast bolus and the fact that no delayed imaging was performed.

The internal architecture of hepatic EHE is better depicted on MRI compared to CT [32]. As seen in our series, lesions are generally hypointense on T1 weighted images and hyperintense on T2 [33]. A target appearance with alternating high and low signal intensity rings similar to that seen on post contrast CT imaging may be visible on T2 weighted imaging as well as on post contrast T1 weighted sequences [34], but this was only seen in one of our patients. Central low signal intensity on T2 weighted sequences is attributed to hemorrhage and/or necrosis; peripheral high signal intensity results from tumor cellular proliferation and adjacent edema [15,30]. Overall, lesions are hypoenhancing relative to normal liver parenchyma and may demonstrate only mild peripheral rim enhancement [28,30]. Dynamic post contrast images show some centripetal filling, and this was seen in the majority of our patients with MRI studies.

The “lollipop” sign may be visible on CT and MRI [4]. This consists

of a hepatic or portal vein tapering and terminating at the periphery or just within a well-defined hypoenhancing lesion. Three dimensional reformat CT and multiplanar MRI are useful in demonstrating this sign. This characteristic sign was seen in 5 of our patients.

On sonography, lesions are predominantly hypoechoic, but occasionally appear iso- to hyperechoic with a hypoechoic rim [35]. On color Doppler intralesional vessels with fast-flow can be seen [36]. On contrast-enhanced sonography, rim-like or heterogeneous enhancement is seen in the arterial phase and hypoenhancement in the portal or delayed venous phases [36].

Within the bones, EHE most commonly involves the axial skeleton and lower limbs. The majority of our patients had disease limited to the axial skeleton. The tibia, femur, and humerus are the most frequently affected long bones [10]. Multifocal disease, which frequently involves the same region or extremity, has been reported in 20–50% of patients [37,38] and was seen in 7/13 of our cohort. Lesions typically appear lytic on radiographs and CT with variable size and zone of transition [10,39], as was seen in almost all of our patients (12/13). Osseous expansion and remodeling are common and cortical destruction may be present; however, periosteal reaction is rare. A small associated soft tissue mass has been reported in up to 40% [40] of patients, but was only seen in one of our patients.

On MRI, lesions usually demonstrate nonspecific low to intermediate T1 and high T2 signal intensity with homogenous enhancement. A peripheral low signal intensity rim has been described on all sequences and was also evident in our review. Despite the vascular nature of this entity, flow voids are not seen [10].

4.1. Limitations

This study has several limitations including its retrospective nature. As a pediatric referral center, our series is biased towards younger patients. Due to the rarity of EHE, only a small number of patients were available for review. In most cases, limited laboratory and clinical data was available, and was provided by a referring institution. Almost all imaging studies were performed at outside institutions with variable imaging parameters. Similarly, the diagnostic biopsies were performed at outside institutions, although available histology was reviewed at BCH. Follow up time was limited and variable. A variety of treatment regimens had been administered to the patients, which may have altered the natural progression of the disease. Because of these limitations, no definite correlation was identified between specific imaging findings and a worse prognosis.

5. Conclusions

Most patients with EHE have multi-organ disease, with lungs, liver and bones most frequently affected. Lung disease is most commonly characterized by multiple nodules. Hepatic lesions demonstrate the most distinctive findings, with peripheral distribution, subcapsular retraction and “lollipop” sign. Osseous lesions are commonly lytic and often restricted to the axial skeleton.

Disclosures

None of the authors have a conflict of interest to disclose.

Funding

This research did not receive any specific grant from funding agencies in the public, commercial, or not-for-profit sectors.

Declaration of Competing Interest

None.

References

[1] Lauffer JM, Zimmermann A, Krahenbuhl L, Triller J, Baer HU. Epithelioid hemangioendothelioma of the liver. A rare hepatic tumor. Cancer 1996;78(11):2318–27.
[2] Lencioni R, Cioni D, Crocetti L, Della Pina C, Bartolozzi C. Magnetic resonance imaging of liver tumors. J Hepatol 2004;40(1):162–71.
[3] Weiss SW, Enzinger FM. Epithelioid hemangioendothelioma: a vascular tumor often mistaken for a carcinoma. Cancer 1982;50(5):970–81. [Oncol Rev. 2014 Oct 13;8(2):259].
[4] Alomari AI. The lollipop sign: a new cross-sectional sign of hepatic epithelioid hemangioendothelioma. Eur J Radiol 2006;59(3):460–4.
[5] Sardaro A, Bardoscia L, Petruzzelli MF, Portaluri M. Epithelioid hemangioendothelioma: an overview and update on a rare vascular tumor.
[6] Rosenberg A, Agulnik M. Epithelioid Hemangioendothelioma: update on diagnosis and treatment. Curr Treat Options Oncol 2018 Mar 15;19(4):19.
[7] Hettmer S, Andrieux G, Hochrein J, et al. Epithelioid hemangioendotheliomas of the liver and lung in children and adolescents. Pediatr Blood Cancer 2017;64(12). Dec.
[8] Tanas MR, Ma S, Jadaan FO, Ng CK, Weigelt B, Reis-Filho JS, et al. Mechanism of action of a WWTR1(TAZ)-CAMTA1 fusion oncoprotein. Oncogene 2016;35(7):929–38. Feb 18.
[9] Lau K, Massad M, Pollak C, et al. Clinical patterns and outcome in epithelioid hemangioendothelioma with or without pulmonary involvement: insights from an internet registry in the study of a rare cancer. Chest 2011;140(5):1312–8.
[10] Ignacio EA, Palmer KM, Mathur SC, Schwartz AM, Olan WJ. Epithelioid hemangioendothelioma of the lower extremity. Radiographics 1999;19(2):531–7.
[11] Mehrabi A, Kashfi A, Fonouni H, et al. Primary malignant hepatic epithelioid hemangioendothelioma: a comprehensive review of the literature with emphasis on the surgical therapy. Cancer 2006;107(9):2108–21.
[12] Lin BT, Colby T, Gown AM, et al. Malignant vascular tumors of the serous membranes mimicking mesothelioma. A report of 14 cases. Am J Surg Pathol 1996;20(12):1431–9.
[13] Totsch M, Dobler G, Feichtinger H, Sandbichler P, Ladurner D, Schmid KW. Malignant hemangioendothelioma of the thyroid. Its immunohistochemical discrimination from undifferentiated thyroid carcinoma. Am J Surg Pathol 1990;14(1):69–74.
[14] Makhlouf HR, Ishak KG, Goodman ZD. Epithelioid hemangioendothelioma of the liver: a clinicopathologic study of 137 cases. Cancer 1999;85(3):562–82.
[15] Lyburn ID, Torreggiani WC, Harris AC, et al. Hepatic epithelioid hemangioendothelioma: sonographic, CT, and MR imaging appearances. AJR Am J Roentgenol 2003;180(5):1359–64.
[16] Dail D, Liebow AA. Intravascular bronchioloalveolar tumor. Am J Pathol 1975(78):6a-7a.
[17] Kim EY, Kim TS, Han J, Choi JY, Kwon OJ, Kim J. Thoracic epithelioid hemangioendothelioma: imaging and pathologic features. Acta Radiol 2011;52(2):161–6.
[18] Cronin P, Arenberg D. Pulmonary epithelioid hemangioendothelioma: an unusual case and a review of the literature. Chest 2004;125(2):789–93.
[19] Mukundan G, Urban BA, Askin FB, Fishman EK. Pulmonary epithelioid hemangioendothelioma: atypical radiologic findings of a rare tumor with pathologic correlation. J Comput Assist Tomogr 2000;24(5):719–20.
[20] Sakamoto N, Adachi S, Monzawa S, et al. High resolution CT findings of pulmonary epithelioid hemangioendothelioma: unusual manifestations in 2 cases. J Thorac Imaging 2005;20(3):236–8.
[21] Dail DH, Liebow AA, Gmelich JT, et al. Intravascular, bronchiolar, and alveolar tumor of the lung (IVBAT). An analysis of twenty cases of a peculiar sclerosing endothelial tumor. Cancer 1983;51(3):452–64.
[22] Crotty EJ, McAdams HP, Erasmus JJ, Sporn TA, Roggli VL. Epithelioid hemangioendothelioma of the pleura: clinical and radiologic features. AJR Am J Roentgenol 2000;175(6):1545–9.
[23] Bahrami A, Allen TC, Cagle PT. Pulmonary epithelioid hemangioendothelioma mimicking mesothelioma. Pathol Int 2008;58(11):730–4.
[24] Hanada N, Namai S, Kobayashi C, et al. Case report of pulmonary epithelioid hemangioendothelioma Nihon Kokyuki Gakkai Zasshi 2003;41(2):144–9.
[25] Luburich P, Ayuso MC, Picado C, Serra-Batlles J, Ramirez JF, Sole M. CT of pulmonary epithelioid hemangioendothelioma. J Comput Assist Tomogr 1994;18(4):562–5.
[26] Miller WJ, Dodd 3rd GD, Federle MP, Baron RL. Epithelioid hemangioendothelioma of the liver: imaging findings with pathologic correlation. AJR Am J Roentgenol 1992;159(1):53–7.
[27] Radin DR, Craig JR, Colletti PM, Ralls PW, Halls JM. Hepatic epithelioid hemangioendothelioma. Radiology 1988;169(1):145–8.
[28] Lin J, Ji Y. CT and MRI diagnosis of hepatic epithelioid hemangioendothelioma. Hepatobiliary Pancreat Dis Int 2010;9(2):154–8.
[29] Zhao XY, Rakhda MI, Habib S, Bihi A, Muhammad A, Wang TL, et al. Hepatic epithelioid hemangioendothelioma: a comparison of Western and Chinese methods with respect to diagnosis, treatment and outcome. Oncol Lett 2014;7(4):977–83. Apr.
[30] Kehagias DT, Moulopoulos LA, Antoniou A, Psychogios V, Vourtsi A, Vlahos LJ. Hepatic epithelioid hemangioendothelioma: MR imaging findings. Hepatogastroenterology 2000;47(36):1711–3.
[31] Fulcher AS, Sterling RK. Hepatic neoplasms: computed tomography and magnetic resonance features. J Clin Gastroenterol 2002;34(4):463–71.
[32] Ros LH, Fernandez L, Villacampa VM, Ros PR. Epithelioid hemangioendothelioma of the liver–characteristics on magnetic resonance imaging: case report. Can Assoc

Radiol J 1999;50(6):387–9.
[33] Amin S, Chung H, Jha R. Hepatic epithelioid hemangioendothelioma: MR imaging findings. Abdom Imaging 2011;36(4):407–14.
[34] Economopoulos N, Kelekis NL, Argentos S, et al. Bright-dark ring sign in MR imaging of hepatic epithelioid hemangioendothelioma. J Magn Reson Imaging 2008;27(4):908–12.
[35] Furui S, Itai Y, Ohtomo K, et al. Hepatic epithelioid hemangioendothelioma: report of five cases. Radiology 1989;171(1):63–8.
[36] Dong Y, Wang WP, Cantisani V, D'Onofrio M, Ignee A, Mulazzani L, et al. Contrast-enhanced ultrasound of histologically proven hepatic epithelioid hemangioendothelioma. World J Gastroenterol 2016;22(19):4741–9. May 21.
[37] Kleer CG, Unni KK, McLeod RA. Epithelioid hemangioendothelioma of bone. Am J Surg Pathol 1996;20(11):1301–11.
[38] Weiss SW, Ishak KG, Dail DH, Sweet DE, Enzinger FM. Epithelioid hemangioendothelioma and related lesions. Semin Diagn Pathol 1986;3(4):259–87.
[39] Errani C, Vanel D, Gambarotti M, Alberghini M, Picci P, Faldini C. Vascular bone tumors: a proposal of a classification based on clinicopathological, radiographic and genetic features. Skeletal Radiol 2012;41(12):1495–507.
[40] Wenger DE, Wold LE. Malignant vascular lesions of bone: radiologic and pathologic features. Skeletal Radiol 2000;29(11):619–31.